ORIGINAL ARTICLE

Respiratory Microbiome Profiles Are Associated With Distinct Inflammatory Phenotype and Lung Function in Children With Asthma

Kim YH[1,2], Park MR[1,2], Kim SY[2,3], Kim MJ[2,4], Kim KW[2,3], Sohn MH[2,3]

[1]Department of Pediatrics, Gangnam Severance Hospital, Seoul, Korea
[2]Institute of Allergy, Department of Biomedical Science, Brain Korea 21 Project for Medical Science, Yonsei University College of Medicine, Seoul, Korea
[3]Department of Pediatrics, Severance Hospital, Seoul, Korea
[4]Department of Pediatrics, Yongin Severance Hospital, Yongin, Korea

J Investig Allergol Clin Immunol 2024; Vol. 34(4): 246-256
doi: 10.18176/jiaci.0918

Abstract

Background: Respiratory microbiome studies have improved our understanding of the various phenotypes and endotypes in heterogeneous asthma. However, the relationship between the respiratory microbiome and clinical phenotypes in children with asthma remains unclear. We aimed to identify microbiome-driven clusters reflecting the clinical features of asthma and their dominant microbiotas in children with asthma.
Methods: Induced sputum was collected from children with asthma, and microbiome profiles were generated via sequencing of the V3-V4 region of the *16S rRNA* gene. Cluster analysis was performed using the partitioning around medoid clustering method. The dominant microbiota in each cluster was determined using linear discriminant effect size analysis. Each cluster was analyzed to identify associations between the dominant microbiota, clinical phenotype, and inflammatory cytokines.
Results: We evaluated 83 children diagnosed with asthma. Among 4 clusters reflecting the clinical characteristics of asthma, cluster 1, dominated by the genera *Haemophilus* and *Neisseria*, demonstrated lower postbronchodilator (BD) forced expiratory volume in 1 second (FEV_1)/forced vital capacity (FVC) than the other clusters and more mixed granulocytic asthma. *Neisseria* correlated negatively with pre-BD and post-BD FEV_1/FVC. *Haemophilus* and *Neisseria* correlated positively with programmed death-ligand (PD-L) 1.
Conclusion: To our knowledge, this study is the first to analyze the relationship between an unbiased microbiome-driven cluster and clinical phenotype in children with asthma. The cluster dominated by *Haemophilus* and *Neisseria* was characterized by fixed airflow obstruction and mixed granulocytic asthma, which correlated with PD-L1 levels. Thus, unbiased microbiome-driven clustering can help identify new asthma phenotypes related to endotypes in childhood asthma.

Key words: Asthma. Children. Cluster analysis. Cytokines. Microbiota. Phenotype.

Resumen

Antecedentes: Los estudios del microbioma respiratorio han favorecido nuestra comprensión de diversos fenotipos y endotipos del asma. Sin embargo, la relación entre el microbioma respiratorio y los fenotipos clínicos en niños con asma sigue sin estar clara. Nuestro objetivo fue identificar, en niños con asma, agrupaciones (clúster) de microbiomas que identifiquen las características clínicas del asma y sus microbiotas dominantes.
Métodos: Se recogió esputo inducido de niños con asma y se generaron perfiles de microbioma mediante secuenciación de la región V3-V4 del gen *16S rRNA*. El análisis de clúster se realizó usando el algoritmo PAM (*Partitioning Around Medoids*). El microbiota dominante en cada clúster se determinó mediante el análisis lineal discriminante. En cada conglomerado se analizó la asociación entre la microbiota dominante, el fenotipo clínico y la citocina inflamatoria.
Resultados: Se evaluaron 83 niños diagnosticados de asma. Entre los cuatro clústeres que reflejaban las características clínicas del asma, el clúster 1, dominado por *Haemophilus* y *Neisseria*, se caracterizaba por tener un volumen espiratorio forzado en 1 segundo (FEV_1) y la capacidad vital forzada (FVC), posbroncodilatador (BD) inferior al de los demás clúster y un asma granulocítica más mixta. *Neisseria* se correlacionó negativamente con el VEF_1/CVF pre y post-BD. *Haemophilus* y *Neisseria* se correlacionaron positivamente con el ligando de muerte programada (PD-L) 1.
Conclusiones: Hasta donde sabemos, este estudio es el primero en analizar la relación entre un clúster no sesgado de microbioma y el fenotipo clínico en niños con asma. El clúster dominado por *Haemophilus* y *Neisseria* mostró obstrucción fija del flujo aéreo y asma granulocítica mixta, que se correlacionó con los niveles de PD-L1. Así pues, la agrupación no sesgada derivada del análisis del microbioma puede ayudar a identificar nuevos fenotipos de asma relacionados con los endotipos en el asma infantil.

Palabras clave: Asma. Niños. Análisis clúster. Citocinas. Microbiota. Fenotipo.

Summary box

- **What do we know about this topic?**
  Unbiased microbiome-driven clustering analysis in childhood asthma suggests that a cluster composed primarily of *Haemophilus* and *Neisseria* displayed fixed airflow obstruction and mixed granulocytic asthma. This observation points to a possible association with programmed death-ligand 1.
- **How does this study impact our current understanding and/or clinical management of this topic?**
  New, microbiome-driven asthma endotyping provides valuable information for an elaborate classification of clinically heterogenous asthma. This approach could enable us to refine management and predict prognosis in children with asthma.

Introduction

Identifying asthma phenotypes and endotypes facilitates a more systematic and differentiated approach for efficient and personalized treatment of asthma, which is heterogeneous and constitutes a syndrome, as opposed to a simple, single disease [1]. The phenotype characterizes the outward clinical features, including the inflammatory cell type and airway obstruction or reversibility; it can be applied intuitively in clinics [2]. Conversely, the endotype provides a comprehensive understanding of the underlying biological mechanisms at the molecular level, including cytokine and microbiome profiling, which can be used to identify disease-specific markers [3]. Identifying the relationship between phenotype and endotype helps to predict the prognosis of heterogeneous asthma and determine the course of treatment [1].

Sputum inflammatory markers, which are characteristic of the asthma phenotype, can be used as a representative tool to understand and explain the diversity and heterogeneity of asthma [4]. Eosinophilic inflammation induced by a heightened type 2 helper T-cell (T_H2) immune response has been suggested as a classical hypothesis for asthma, whereas neutrophil inflammation is characteristic of nonatopic asthma, which is resistant to corticosteroids [5,6]. The respiratory microbiome is an important tool for determining the asthma endotype and thus helping us to understand the mechanism underlying the development and exacerbation of asthma, which may be related to the sputum inflammatory phenotype [7,8]. Early asymptomatic colonization by *Streptococcus* was suggested as a strong predictor of onset of asthma [9]. Gram-negative microbes and airway microbiome composition and diversity could be related to asthma exacerbation [10]. Respiratory microbiome diversity is reduced in neutrophilic asthma, and opportunistic microbes, such as the genus *Haemophilus*, are replaced. These findings may be associated with severe asthma [11]. Unbiased clustering of the microbiome may reflect the clinical characteristics and severity of asthma [12].

Unlike adult asthma, childhood asthma is characterized by allergic comorbidities, including atopic dermatitis and food allergy associated with the allergic march, which, in turn, is thought to be associated mainly with the T_H2 immune response and eosinophilic inflammation [13]. However, neutrophilic asthma has recently been reported to be very frequent in children, possibly owing to bacterial and/or viral infection [14]. Given the limitation of sampling in children compared with adults, few studies have assessed the relationship between the respiratory microbiome and clinical phenotypes in children with asthma [15].

Therefore, we aimed to classify and characterize the respiratory microbiome in children with asthma using unbiased clustering methods and to evaluate the relationship between these microbiome features and clinical phenotypes, including sputum inflammatory phenotype, bronchial hyperresponsiveness (BHR), bronchodilator responsiveness (BDR), and airway obstruction. We also aimed to evaluate inflammatory cytokines to elucidate the mechanisms by which microbiome-driven inflammation can affect specific phenotypes.

Methods

Participants

We screened children who visited the Severance Children's Hospital for an asthma work-up or treatment from January 2015 to December 2018. The children underwent spirometry, sputum induction, and blood sampling at the first visit, followed by the challenge test at the second visit.

Children with typical asthma symptoms, such as recurrent cough or dyspnea, shortness of breath, and chest tightness, underwent spirometry with a bronchodilator (BD) and the bronchoprovocation test. Asthma was diagnosed based on the Global Initiative for Asthma guidelines if a 20% reduction in the forced expiratory volume in 1 second (FEV_1) occurred in response to a provocative concentration of inhaled methacholine (provocholine, PC_{20} <10 mg/mL) or BD response, which was verified as a >12% increase in FEV_1 after inhalation of albuterol 200 μg [16]. We excluded children with the following symptoms: 1) fever, myalgia, purulent sputum, persistent wet cough, and runny and congested nose for 10 days, as found in differential diagnoses of asthma, including acute respiratory infection; and 2) cough when feeding or vomiting easily, as in cardiac murmur or aspiration [16]. Children with acute asthma exacerbation in the previous 4 weeks requiring systemic corticosteroids or increased use of inhaled corticosteroids were also excluded [17].

We used the Pharmacia CAP assay (Thermo Fisher Scientific) to measure serum specific immunoglobulin E (IgE) levels for the following common inhalant allergens in Korea: 2 types of dust mites (*Dermatophagoides pteronyssinus*

and *Dermatophagoides farinae*); cat and dog epithelium; cockroach; mold; and pollen allergens, including *Alternaria*, birch, mugwort, Japanese hop, and ragweed. Atopy was defined as specific IgE ≥0.35 kU_A/L for more than 1 allergen.

Sputum Induction and Processing

After washing their mouths thoroughly with water, all children inhaled 3% saline solution nebulized in an ultrasonic nebulizer (NE-U12, Omron Co.) at maximum output at room temperature and were encouraged to cough deeply at 3-minute intervals thereafter. For the cell count and microbiome analysis, sputum samples were stored at 4°C for no more than 2 hours before further processing. A fraction of the sample was diluted with phosphate-buffered saline (PBS) containing 10 mmol/L dithiothreitol (WAKO Pure Chemical Industries Ltd). For cytokine analysis, another fraction of the sample was vortexed gently at room temperature for 20 minutes after dilution with PBS containing dithiothreitol 10 mmol/L. Sputum aliquots for microbiome and cytokine analysis were stored at –20°C immediately after collection and then at –70°C within 12 hours to maintain acceptable quality for microbiome analysis [18].

Sputum samples were classified as eosinophilic (>2.5% eosinophils), neutrophilic (>54% neutrophils), mixed granulocytic (>2.5% eosinophils, >54% neutrophils), or paucigranulocytic (≤2.5% eosinophils, ≤54% neutrophils) [19].

This study was approved by the Institutional Review Board of Severance Hospital (protocol no. 4-2004-0036). Written informed consent was obtained from the participants and their parents.

DNA Extraction, Polymerase Chain Reaction Amplification, and Sequencing

DNA extraction, polymerase chain reaction (PCR) amplification, and sequencing were performed concurrently for all samples stored at –70°C during the recruitment period (2015-2018). For microbiome analysis, total DNA was extracted from a fraction of the sputum sample using the FastDNA® SPIN Kit for Soil (MP Biomedicals) in accordance with the manufacturer's instructions. The ratio of absorbance was calculated at 260 nm and 280 nm (A260/A280) to assess the purity of DNA. The A260/A280 values of all samples were >2.0, indicating that the purity of DNA was acceptable [20]. Polymerase chain reaction (PCR) amplification was performed using fusion primers targeting the V3-V4 regions of the *16S rRNA* gene with the extracted DNA. For bacterial amplification, fusion primers of 341F (5′-AATGATACGGCGACCACCGAGATCTACAC-XXXXXXXXX-TCGTCGGCAGCGTC-AGATGTGTATAAGAGACAG-CCTACGGGNGGCWGCAG-3′; underlined sequence indicates the target region primer) and 805R (5′-CAAGCAGAAGACGGCATACGAGAT-XXXXXXXX-GTCTCGTGGGCTCGG-AGATGTGTATAAGAGACAG-GACTACHVGGGTATCTAATCC-3′) were constructed in the following order: P5 (P7) graft binding, i5 (i7) index, Nextera consensus, Sequencing adaptor, and Target region sequence.

Amplifications were performed under the following conditions: initial denaturation at 95°C for 3 minutes, followed by 25 cycles of denaturation at 95°C for 30 seconds, primer annealing at 55°C for 30 seconds, extension at 72°C for 30 seconds, and final elongation at 72°C for 5 minutes.

The PCR product was confirmed using 1% agarose gel electrophoresis and visualized using a Gel Doc system (Bio-Rad). The amplified products were purified with Clean PCR (CleanNA). Equal concentrations of purified products were pooled, and short fragments (nontarget products) were removed using Clean PCR (CleanNA). The quality and product size were assessed using the Agilent 2100 Bioanalyzer system (Agilent) with a DNA 7500 chip. Mixed amplicons were pooled and sequenced at Chunlab, Inc. (Seoul, Korea), with the Illumina MiSeq Sequencing system (Illumina), according to the manufacturer's instructions.

Microbiome Data Analysis

Raw reads were processed by performing a quality check and filtering low-quality (<Q25) reads using Trimmomatic ver. 0.32 [21]. Once the quality check was complete, paired-end sequence data were merged using the fastq_mergepairs command of VSEARCH version 2.13.4 [22] with default parameters. Primers were trimmed using the alignment algorithm of Myers and Miller [23] at a similarity cut-off of 0.8. Nonspecific amplicons that did not encode *16S rRNA* were detected using nhmmer [24] in the HMMER software package ver. 3.2.1 with hmm profiles. Unique reads were extracted, and redundant reads were clustered with unique reads using the derep_full length command of VSEARCH [22]. The EzBioCloud *16S rRNA* database [25] was used for the taxonomic assignment based on the usearch_global command of VSEARCH [22], followed by more precise pairwise alignment [23]. Chimeric reads were filtered based on <97% similarity by reference-based chimeric detection using the UCHIME algorithm [26] and the nonchimeric *16S rRNA* database from EzBioCloud. After chimeric filtering, reads that were not identified to the species level (with <97% similarity) in the EzBioCloud database were compiled, and de novo clustering was performed using the cluster_fast command [22] to generate additional operational taxonomic units (OTUs). OTUs with single reads (singletons) were omitted from further analysis.

Cytokine Analysis

Cytokine analysis of sputum was performed using a human fixed immunotherapy discovery magnetic panel-24 plex kit (Magnetic Luminex® Performance Assay multiplex kit, R&D Systems). This kit was used to analyze CD40, granulocyte-macrophage colony-stimulating factor, granzyme B, interferon α, interferon γ, interleukin (IL) 1α, IL-1β, IL-1Ra, IL-2, IL-4, IL-6, IL-8, IL-10, IL-12p70, IL-13, IL-15, IL-17A, IL-33, C-X-C motif chemokine 10, monocyte chemoattractant protein-1, macrophage inflammatory proteins (MIP)-1α, MIP-1β, programmed death-ligand (PD-L) 1, and tumor necrosis factor α.

Microbiome Data Analysis for the Clustered Groups

Samples were clustered using species-level abundance data with partitioning around medoid (PAM) clustering based on

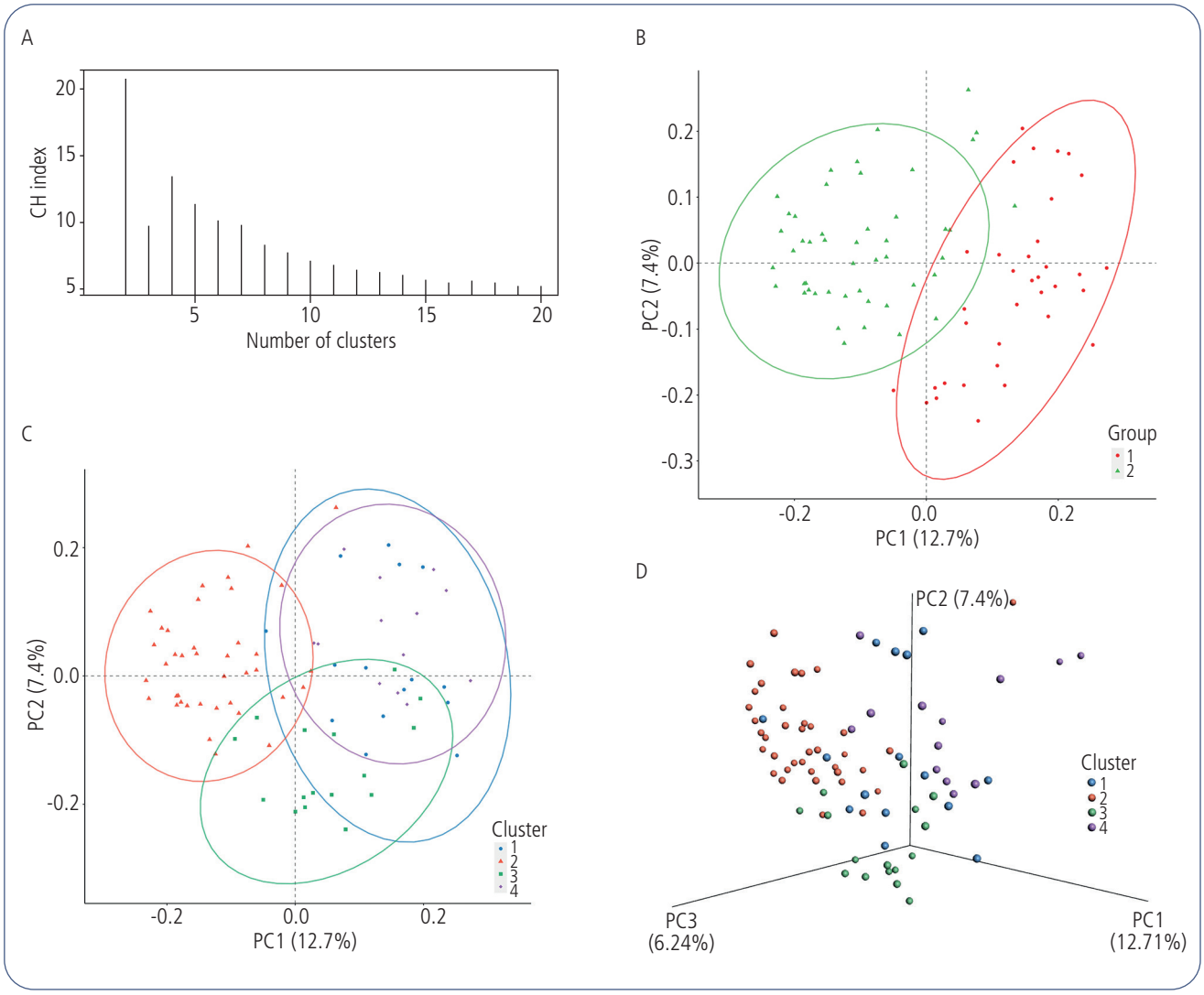

Figure 1. A, Calinski–Harabasz (CH) index according to cluster number using the partitioning around medoid clustering method based on Jensen–Shannon divergence at the species level. B, Two-dimensional (2D) principal coordinate analysis (PCoA) plot for cluster 2. C, 2D PCoA plot for cluster 4. D, Three-dimensional PCoA plot for cluster 4.

the Jensen-Shannon divergence [27]. The Calinski–Harabasz (CH) index was calculated according to the number of clusters and used to determine the optimal number of clusters [28]. The resulting clusters were visualized using R with package ade4 for principal coordinate analysis (PCoA) based on the Jensen-Shannon divergence [29].

Linear discriminant analysis (LDA) effect size was used to discover microbiota as a biomarker related to each cluster. The clusters showed a significant difference in the analysis using the Kruskal-Wallis H test. Significant biomarkers were obtained with an LDA score >4.0 and P value <.05 in the pairwise comparison using the Mann-Whitney test and Bonferroni adjustment [30]. The resulting biomarkers were visualized using GraPhlAn for cladogram and the statistical package R (R version 3.2.5.; Institute for Statistics and Mathematics; www.R-project.org) with the package *ggplot* for boxplot using the Kruskal-Wallis H test [31].

Statistical Analysis

The clusters were defined using PAM clustering and the CH index. In order to evaluate clinical characteristics across the clusters, we compared the participants' demographics, the pulmonary function parameters, such as the airway obstruction index (FEV_1, FEV_1/forced vital capacity [FVC]), fixed airway obstruction index (post-BD FEV_1, post-BD FEV_1/FVC), airway hyperresponsiveness, and BD response, and sputum inflammatory phenotype across the clusters. Continuous variables were analyzed using the t test, Mann-Whitney test, 1-way analysis of variance, or Kruskal-Wallis test. Categorical variables were analyzed using the χ^2 or Fisher exact test. Post hoc analysis with the Bonferroni correction was performed if a significant difference was observed between the 4 clusters. The Spearman rank correlation was used to assess the relationship between the microbiota as a biomarker

for the clusters compared with inflammatory cytokines and pulmonary function parameters. *P* values <.05 were considered statistically significant. The analysis was performed using IBM SPSS Statistics for Windows, Version 23.0 (IBM Corp.) and R (R version 3.2.5; Institute for Statistics and Mathematics; www.R-project.org).

Results

Clinical Characteristics Across the Clusters

We evaluated 83 children diagnosed with asthma (median age, 7.5 years; 31.3% boys). Most children (approximately 83%) were atopic.

According to the number of clusters, defined using the PAM clustering method, a higher CH index was obtained in 2 and 4 clusters than in other numbers of clusters (Figure 1A), which were well separated in the PCoA plots (Figures 1B-D).

We compared the clinical characteristics of the participants across the 2 and the 4 clusters. The 4 clusters showed significantly different clinical characteristics, including inflammatory phenotype (*P*=.007) and pulmonary function parameters (Table), whereas the 2 clusters did not show any significantly different clinical characteristics (Supplementary Table 1). Post-BD FEV_1/FVCs (*P*=.020) differed significantly across the 4 clusters; however, the difference in pre-BD FEV_1/FVC was not statistically significant (*P*=.060). Therefore, we comprehensively evaluated the clinical characteristics and microbiome profile in the 4 clusters to identify microbiotas as meaningful biomarkers related to clinical characteristics, such as inflammatory phenotype and pulmonary function parameters.

Sputum Inflammatory Phenotype and Pulmonary Function Parameters Across the Clusters

We performed a post hoc analysis to identify the clusters that differed significantly in inflammatory phenotype. Only clusters 1 and 2 exhibited a significant difference with multiple corrections (Figure 2A). A post hoc analysis was also performed to identify which inflammatory phenotype differed significantly in clusters 1 and 2. Given the absence of a significantly different inflammatory phenotype that could explain the difference between clusters 1 and 2, the difference in inflammatory phenotype between these 2 clusters was evaluated without a Bonferroni correction (Figure 2B). This explorative investigation revealed differences in the mixed granulocytic and paucigranulocytic types in clusters 1 and 2 (Figure 2B).

Cluster 1 had a lower post-BD FEV_1/FVC than the other clusters (Figure 2C). In a pairwise comparison between 2 clusters, the post-BD FEV_1/FVC of cluster 1 was significantly lower than that of cluster 2 (*P*=.031) after the Bonferroni correction.

In summary, cluster 1 had a lower post-BD FEV_1/FVC, indicating fixed airflow obstruction and more mixed granulocytic and paucigranulocytic asthma.

Dominant Microbiotas in the Clusters

The *16S rRNA* analytic method has limitations in identifying an individual microbe at the species level when applied with only partial amplicons [8]. Therefore, the abundance of the microbiotas was analyzed up to the genus level (Supplementary Fig. 1) and compared at the genus level between the clusters (Figure 3) at *P*<.05 using the Kruskal-Wallis H test to identify

Table. Patient Characteristics Across the 4 Clusters (N=83).

	Total (N=83)	Cluster 1 (n=15)	Cluster 2 (n=39)	Cluster 3 (n=16)	Cluster 4 (n=13)	*P* value
Age, y	7.5 (6.5-9.7)	8.2 (6.5-10.4)	7.5 (6.3-9.7)	8.9 (7.5-10.7)	6.5 (5.7-7.9)	.020
Male sex, No. (%)	26 (31.3)	14 (93.3)	24 (61.5)	9 (56.3)	10 (76.9)	.081
Atopy, No. (%)	29 (82.9)	10 (66.7)	31 (79.5)	15 (93.8)	11 (84.6)	.282
Sputum inflammatory phenotype, No. (%)						
Eosinophilic	27 (32.5)	3 (20.0)	18 (46.2)	1 (6.3)	5 (38.5)	.007
Neutrophilic	32 (38.6)	2 (13.3)	15 (38.5)	10 (62.5)	5 (38.5)	
Mixed	13 (15.7)	6 (40.0)	4 (10.3)	2 (12.5)	1 (7.7)	
Paucigranulocytic	11 (13.3)	4 (26.7)	2 (5.1)	3 (18.8)	2 (15.4)	
Pulmonary function parameters						
Mean (SD) FEV_1, % predicted	96.8 (16.2)	92.4 (16.0)	98.4 (16.2)	98.5 (15.5)	94.8 (17.8)	.610
FEV_1/FVC	81.4 (74.1-85.5)	0.76 (0.70-0.81)	0.83 (0.74-0.86)	0.84 (0.80-0.88)	0.80 (0.71-0.84)	.060
Mean (SD) post-BD FEV_1, % predicted	105.7 (15.8)	101.3 (18.5)	108.1 (15.1)	105.1 (14.6)	104.3 (16.2)	.540
Post-BD FEV_1/FVC	85.3 (80.8-91.1)	80.5 (75.8-86.3)	88.0 (83.0-91.3)	86.5 (83.0-91.8)	84.5 (77.3-89.0)	.020
BDR to assess Δ FEV_1	29 (34.9)	7 (46.7)	14 (35.9)	4 (25.0)	4 (30.8)	.633
BHR to assess challenge test	62 (74.7)	8 (57.1)	32 (84.2)	12 (75.0)	10 (83.3)	.204

Abbreviations: BD, bronchodilator; BDR, bronchodilator response; BHR, bronchial hyperresponsiveness; Δ, change before and after bronchodilator; FEV_1, forced expiratory volume in 1 second; FVC, forced vital capacity.

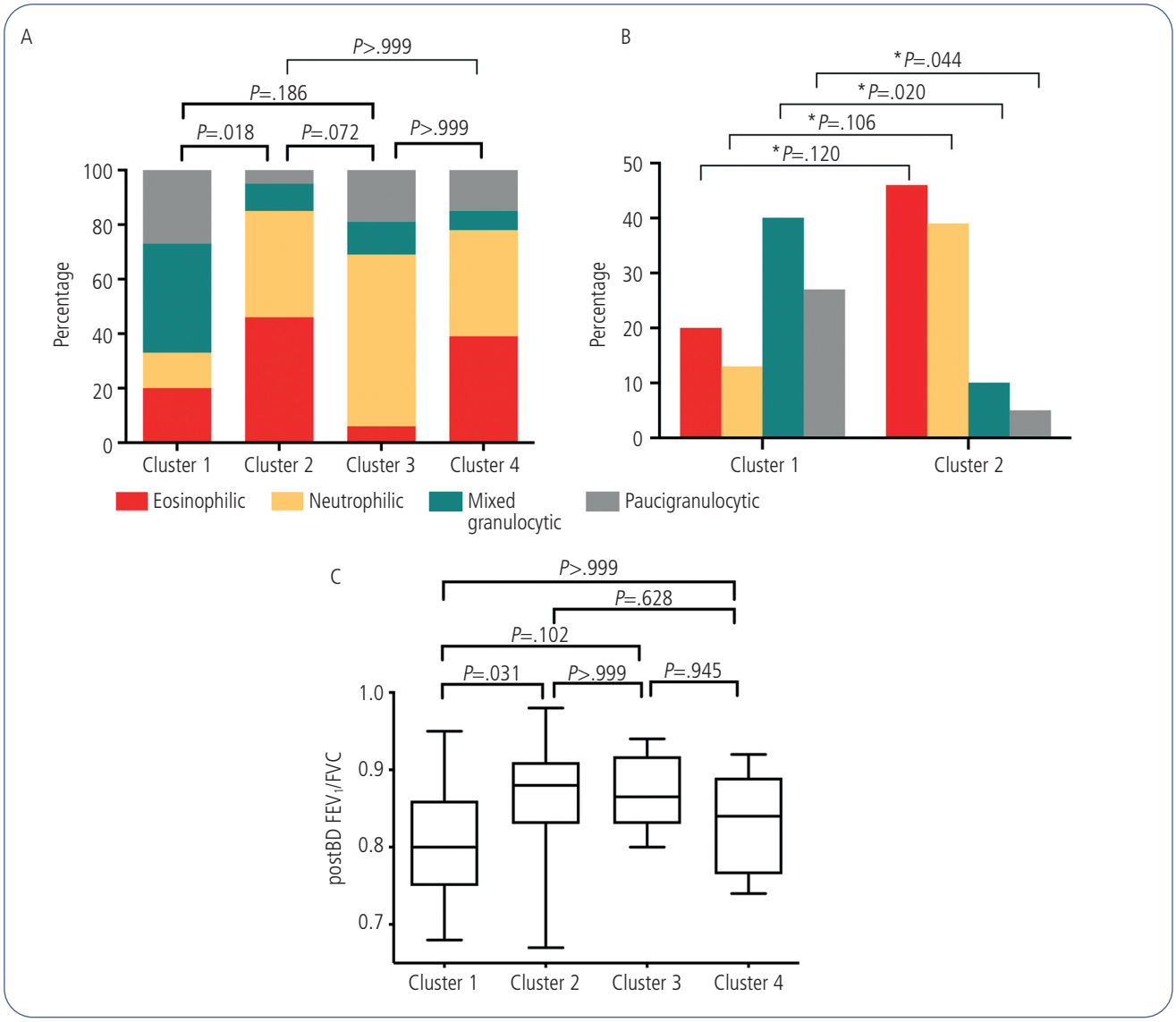

Figure 2. A, Comparison of the sputum inflammatory phenotype across the clusters. B, Comparison of the sputum inflammatory phenotype in clusters 1 and 2. C, Post-bronchodilator (BD) forced expiratory volume in 1 second (FEV_1)/forced vital capacity (FVC) across the clusters. The *P* value was calculated using post hoc analysis with Bonferroni correction. **P* was calculated using post hoc analysis without a Bonferroni correction for exploratory purposes.

the dominant microbiotas related to each cluster. Microbiotas were selected at the genus level with an LDA score >4.0, as seen in the LDA histogram and cladogram in Figure 4. The predominance was as follows: *Neisseria* and *Haemophilus* in cluster 1; *Prevotella*, *Veillonella*, and *Actinomyces* in cluster 2; *Streptococcus* and *Granulicatella* in cluster 3; and *Ralstonia* in cluster 4.

Correlation Between Microbiota and Inflammatory Cytokines and Pulmonary Function

The correlation between the prominent genera and inflammatory cytokines was analyzed (Supplementary Table 2). Samples from 63 of the 83 participants were available for analysis of inflammatory cytokines. Since cluster 1 had a more mixed granulocytic type and fixed airway obstruction, and *Neisseria* and *Haemophilus* were predominant in cluster 1, we focused on the cytokine that correlated significantly with these 2 genera. Only PD-L1 had a meaningful correlation with both microbes (r=0.445, *P*=.016 for *Neisseria*; r=0.450, *P*=.014 for *Haemophilus*).

We analyzed the correlation between the predominant genera, including *Neisseria* and *Haemophilus*, and the less abundant genera, including *Streptococcus*, in cluster 1 and compared the results with the pre-BD and post-BD FEV_1/FVC indices (Figure 5). Only *Neisseria* correlated negatively with pre-BD FEV_1/FVC (r=–0.227, *P*=.039) and post-BD FEV_1/FVC (r=–0.227, *P*=.039), whereas no significant correlation was detected between the other microbiotas and the pre-BD and post-BD FEV_1/FVC indices.

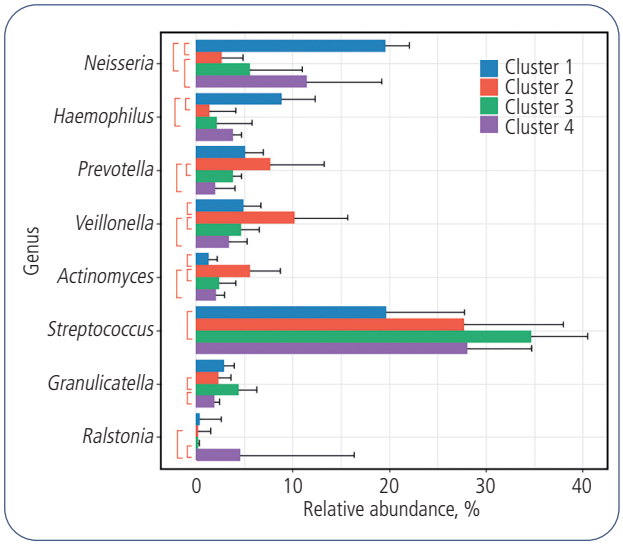

Figure 3. Comparison of microbiota at the genus level among the clusters with *P*<.001 in the Kruskal–Wallis H test. The red lines represent *P*<.05 in the pairwise comparison using the Mann-Whitney test and Bonferroni correction.

Discussion

An unbiased microbiome profile clustering method used in children with asthma revealed that the cluster with abundant *Neisseria* and *Haemophilus* demonstrated fixed airflow obstruction based on the post-BD FEV_1/FVC index and a more mixed granulocytic phenotype. The pre-BD and post-BD FEV_1/FVC indices decreased, with an increase in the relative abundance of *Neisseria*, indicating that *Neisseria* could be related to airway obstruction in childhood asthma. *Neisseria* and *Haemophilus* correlated positively with PD-L1 levels, suggesting that they could affect fixed airflow obstruction and mixed granulocytic phenotype in relation to PD-L1 in childhood asthma.

Microbiome study is used for asthma endotyping, which defines the subtypes of heterogenous asthma based on the underlying pathologic mechanisms [7]. Previous studies on microbiome data are limited to a supervised approach using known clinical phenotypes and do not address independent microbiome-driven subtyping [11,32,33]. A recent microbiome study in adult asthma suggested the clinical significance of unbiased clustering based on microbiome profiles alone [12]. We applied this unbiased clustering method in children with asthma, and the cluster showed a significant association with clinical characteristics, including fixed airflow obstruction and the mixed granulocytic type. Thus, the unbiased cluster analysis of the airway microbiome was clinically meaningful in childhood asthma.

Haemophilus, a pathogenic microbe found in airway dysbiosis, is considered a major pathogenic microorganism in asthma attacks [10]. It is highly abundant in the neutrophilic phenotype of severe asthma [11] and is prominent in eosinophilic asthma [33]. The relevance of *Neisseria* in eosinophilic asthma is debatable [32,33]. As both neutrophilic and eosinophilic inflammatory processes play a role in asthma related to the T_H1 and T_H2 immune responses and many debatable results have been reported [13,14], it is reasonably acceptable that cluster 1 is characterized by more mixed granulocytic asthma.

PD-L1, which correlated significantly and positively with *Neisseria* and *Haemophilus* in our study, may strengthen T_H2 inflammation and increase airway hyperresponsiveness in asthma; however, it can suppress CD8 T-cell immunity, preventing the clearance of infected pathogens from the perspective of acute infection [34,35]. The dual roles of PD-L1 in asthma, including strengthening T_H2 inflammation and weakening innate immunity from infected pathogens, can explain its contribution to asthma exacerbation [10]. These dual roles can also contribute to eosinophilic inflammation through a T_H2 immune response and to neutrophilic inflammation

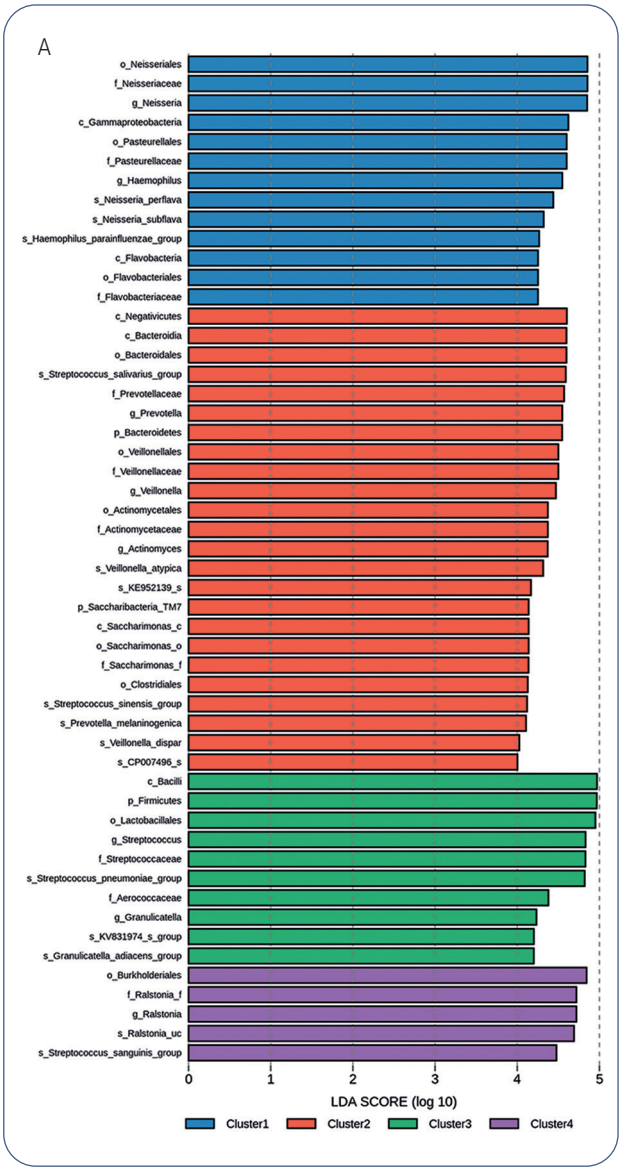

Figure 4. A, Linear discriminant analysis (LDA) effect size analysis across the 4 clusters with *P*<.05 and an LDA score >4.0.

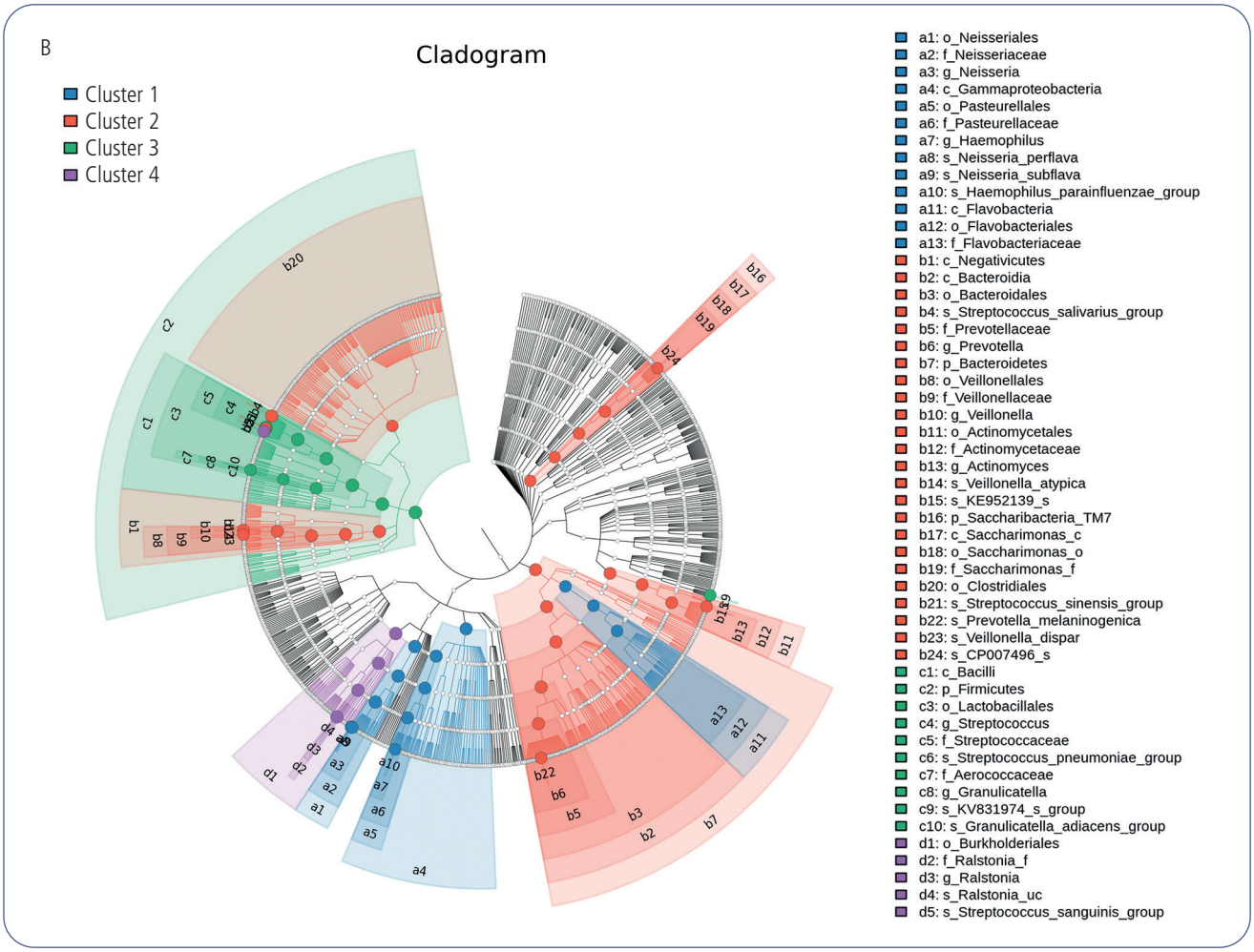

Figure 4. B, Cladogram showing differentially abundant taxa according to each cluster. *Haemophilus parainfluenzae* group (*Haemophilus influenzae*, *Haemophilus aegyptius*, and unclassified microbes), *Streptococcus salivarius* group (*Streptococcus salivarius* subsp. *salivarius*, *Streptococcus thermophilus*, *Streptococcus vestibularis*, and unclassified microbes), *Streptococcus sinensis* group (*Streptococcus sinensis* and unclassified microbes), *Streptococcus pneumoniae* group (*Streptococcus pneumonia*, *Streptococcus oralis* subsp. *oralis*, *Streptococcus oralis* subsp. *tigurinus*, *Streptococcus oralis* subsp. *dentisani*, *Streptococcus mitis*, *Streptococcus infantis*, *Streptococcus pseudopneumoniae*, *Streptococcus timonensis*, and unclassified microbes), *Streptococcus sanguinis* group (*Streptococcus sanguinis* and unclassified microbes), and *Granulicatella adiacens* group (*Granulicatella adiacens* and unclassified microbes).

through recurrent infection, leading to a more mixed phenotype in the cluster in which the genera *Neisseria* and *Haemophilus* were dominant in our study.

There are few studies on fixed airflow obstruction in children, a characteristic of chronic obstructive pulmonary disease (COPD), which can be an index of severe asthma when accompanied by asthma in adults [36-38]. It generally develops owing to airway remodeling driven by chronic inflammation [36,39]. Frequent asthma exacerbation can be a risk factor for fixed airflow obstruction in children with asthma [40], and infections are the leading cause of asthma exacerbations in children [41,42]. In this study, cluster 1 was characterized by a mixed granulocytic phenotype, causing fixed airflow obstruction owing to increased inflammatory reactions triggered by eosinophilic and neutrophilic inflammatory responses [43]. This finding is supported by previous reports revealing that overlapping inflammatory pathways, which present as elevated eosinophil and neutrophil values, might be detrimental to lung function [44].

Neisseria and *Haemophilus* were the predominant genera in cluster 1, which was associated with fixed airflow obstruction; in contrast, *Prevotella, Veillonella*, and *Actinomyces* were the predominant genera in cluster 2, which was associated with favorable lung function. This finding is in line with that of previous reports showing that airway microbial dysbiosis with overgrowth of opportunistic pathogens and lower normal airway microbes can develop simultaneously and aggravate asthma [11]. *Neisseria* correlated independently with airflow limitation parameters, consistent with previous findings, and the increased prevalence of *Neisseria* due to rhinovirus infection can induce the immunomodulatory properties of dendritic cells and proinflammatory cytokines [45,46], which might affect pulmonary function. This possible explanation is justified in children, who are increasingly exposed to respiratory virus infections [47].

Cluster 2, with favorable lung function, was characterized by a predominance of *Prevotella, Veillonella*, and *Actinomyces*. *Prevotella* is more predominant in controls and infants

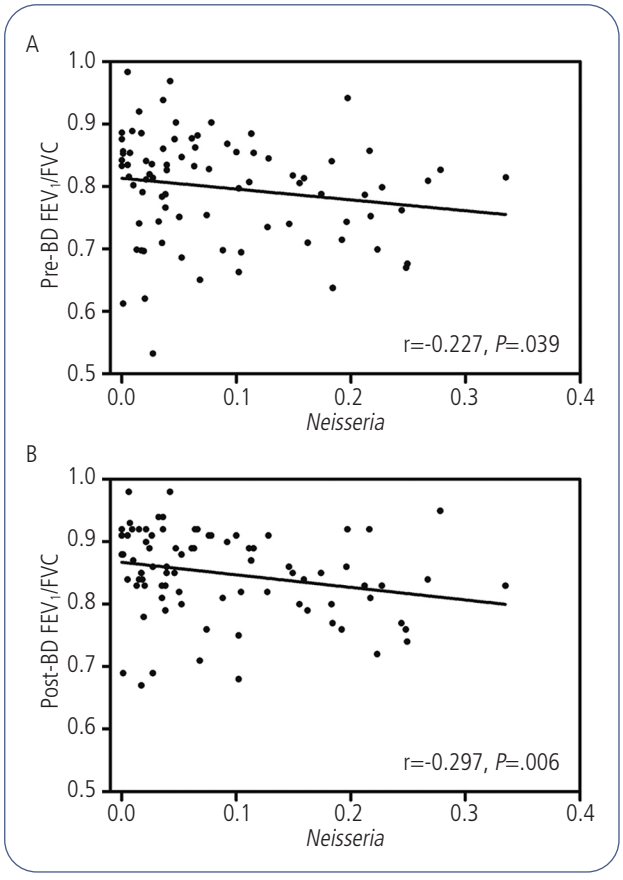

Figure 5. Correlation between pre-BD and post-BD FEV_1/FVC vs *Neisseria*
BD indicates bronchodilator; FEV*1*, forced expiratory volume in 1 second; FVC, forced vital capacity.

without wheezing than in patients and infants with asthma or COPD and wheezing [48]. *Prevotella* was thought to reduce pathologic *Haemophilus influenzae*–induced IL-12p70 [49] and neutrophilic airway inflammation [50]. However, the presence of *Prevotella* and *Veillonella* at 1 month of age was associated with the incidence of asthma at 6 years of age [51]. *Actinomyces* was less abundant in acute asthma exacerbation than in stable asthma [10]. It was also less abundant in neutrophilic asthma, which is considered a severe type of asthma [11].

Cluster 3 included older patients and more women than the other clusters. *Streptococcus* and *Granulicatella* were predominant in cluster 3. *Streptococcus* was the most abundant genus in our study, as reported elsewhere [52], and is an early marker for predicting asthma during later childhood in infants [9]. In contrast, cluster 4 included younger patients, and *Ralstonia* was predominant in cluster 3. *Ralstonia*, classified as pathologic *Pseudomonas* until recently, was reported to be positively correlated with pyruvic acid, which has a crucial protective role in IgE production in response to allergens [53]. Airway microbiomes exhibit distinct features according to age and sex; however, this finding has not been adequately addressed [52,54,55].

Our study has several limitations. First, the number of patients for evaluation of the 4 clusters was small. Second, we could not evaluate the 2 clusters with the optimal CH index, as these clusters could not account for the clinical characteristics. Third, we could not collect detailed clinical information, including the degree of control of asthma, asthma duration, drug usage, and the frequency of acute exacerbation. Despite these limitations, to our knowledge, this study is the first to analyze the relationship between an unbiased microbiome-driven cluster and clinical phenotype in children with asthma. In addition, it is significant that the characteristics of fixed airflow obstruction and mixed granulocytic asthma in children, which were sporadically reported, were assessed through the relationship between the microbiome and inflammatory cytokines. The findings of this study provide insights into the effect of the airway microbiome on lung function, which has not been addressed [42].

In conclusion, the microbiome-driven unbiased clustering method can help to identify new endotype-related asthma phenotypes in childhood asthma. Our findings suggested that the cluster dominated by *Haemophilus* and *Neisseria* found through this method is characterized by fixed airflow obstruction and mixed granulocytic asthma, which can be related to PD-L1. Thus, new asthma endotyping driven by the airway microbiome can provide valuable information for determining precise management modalities and predicting prognosis in children with asthma.

Funding

This research was supported by the VITAL-Korea project from the Ministry of Health and Welfare (MoHW) of the Korean Government (grant number: HV22C0259) and the Basic Science Research Program through the National Research Foundation of Korea (NRF), which is funded by the Ministry of Science, ICT, Future Planning (grant number: NRF-2018R1A5A2025079, NRF-2021R1C1C1011294 and RS-2023-00208036).

Conflicts of Interest

The authors declare that they have no conflicts of interest.

References

1. Kaur R, Chupp G. Phenotypes and endotypes of adult asthma: Moving toward precision medicine. J Allergy Clin Immunol. 2019;144:1-12.
2. Skloot GS. Asthma phenotypes and endotypes: a personalized approach to treatment. Curr Opin Pulm Med. 2016;22:3-9.
3. Ghosh A, Saha S. Meta-analysis of sputum microbiome studies identifies airway disease-specific taxonomic and functional signatures. J Med Microbiol. 2022;72.
4. Seys SF. Role of sputum biomarkers in the management of asthma. Curr Opin Pulm Med. 2017;23:34-40.
5. Akar-Ghibril N, Casale T, Custovic A, Phipatanakul W. Allergic Endotypes and Phenotypes of Asthma. J Allergy Clin Immunol Pract. 2020;8:429-40.
6. Moore WC, Hastie AT, Li X, Li H, Busse WW, Jarjour NN, et al. Sputum neutrophil counts are associated with more severe asthma phenotypes using cluster analysis. J Allergy Clin Immunol. 2014;133:1557-63.e5.

7. Valverde-Molina J, García-Marcos L. Microbiome and Asthma: Microbial Dysbiosis and the Origins, Phenotypes, Persistence, and Severity of Asthma. Nutrients. 2023;15:486.
8. Zubeldia-Varela E, Barker-Tejeda TC, Obeso D, Villaseñor A, Barber D, Pérez-Gordo M. Microbiome and Allergy: New Insights and Perspectives. J Investig Allergol Clin Immunol. 2022;32:327-44.
9. Teo SM, Mok D, Pham K, Kusel M, Serralha M, Troy N, et al. The infant nasopharyngeal microbiome impacts severity of lower respiratory infection and risk of asthma development. Cell Host Microbe. 2015;17:704-15.
10. Kim YH, Jang H, Kim SY, Jung JH, Kim GE, Park MR, et al. Gram-negative microbiota is related to acute exacerbation in children with asthma. Clin Transl Allergy. 2021;11:e12069.
11. Taylor SL, Leong LEX, Choo JM, Wesselingh S, Yang IA, Upham JW, et al. Inflammatory phenotypes in patients with severe asthma are associated with distinct airway microbiology. J Allergy Clin Immunol. 2018;141:94-103.e15.
12. Abdel-Aziz MI, Brinkman P, Vijverberg SJH, Neerincx AH, Riley JH, Bates S, et al. Sputum microbiome profiles identify severe asthma phenotypes of relative stability at 12 to 18 months. J Allergy Clin Immunol. 2021;147:123-34.
13. Douwes J, Gibson P, Pekkanen J, Pearce N. Non-eosinophilic asthma: importance and possible mechanisms. Thorax. 2002;57:643-8.
14. McDougall CM, Helms PJ. Neutrophil airway inflammation in childhood asthma. Thorax. 2006;61:739-41.
15. Shah R, Bunyavanich S. The airway microbiome and pediatric asthma. Curr Opin Pediatr. 2021;33:639-47.
16. Bateman ED, Hurd SS, Barnes PJ, Bousquet J, Drazen JM, FitzGerald JM, et al. Global strategy for asthma management and prevention: GINA executive summary. Eur Respir J. 2008;31:143-78.
17. Fergeson JE, Patel SS, Lockey RF. Acute asthma, prognosis, and treatment. J Allergy Clin Immunol. 2017;139:438-47.
18. Cuthbertson L, Rogers GB, Walker AW, Oliver A, Hafiz T, Hoffman LR, et al. Time between collection and storage significantly influences bacterial sequence composition in sputum samples from cystic fibrosis respiratory infections. J Clin Microbiol. 2014;52:3011-6.
19. Fleming L, Tsartsali L, Wilson N, Regamey N, Bush A. Sputum inflammatory phenotypes are not stable in children with asthma. Thorax. 2012;67:675-81.
20. Koetsier G, Cantor E. A practical guide to analyzing nucleic acid concentration and purity with microvolume spectrophotometers. New England Biolabs Inc. 2019:1-8.
21. Bolger AM, Lohse M, Usadel B. Trimmomatic: a flexible trimmer for Illumina sequence data. Bioinformatics. 2014;30:2114-20.
22. Rognes T, Flouri T, Nichols B, Quince C, Mahé F. VSEARCH: a versatile open source tool for metagenomics. PeerJ. 2016;4:e2584.
23. Myers EW, Miller W. Optimal alignments in linear space. Comput Appl Biosci. 1988;4:11-7.
24. Wheeler TJ, Eddy SR. nhmmer: DNA homology search with profile HMMs. Bioinformatics. 2013;29:2487-9.
25. Yoon SH, Ha SM, Kwon S, Lim J, Kim Y, Seo H, et al. Introducing EzBioCloud: a taxonomically united database of 16S rRNA gene sequences and whole-genome assemblies. Int J Syst Evol Microbiol. 2017;67:1613-7.
26. Edgar RC, Haas BJ, Clemente JC, Quince C, Knight R. UCHIME improves sensitivity and speed of chimera detection. Bioinformatics. 2011;27:2194-200.
27. Arumugam M, Raes J, Pelletier E, Le Paslier D, Yamada T, Mende DR, et al. Enterotypes of the human gut microbiome. Nature. 2011;473:174-80.
28. Caliński T, Harabasz J. A dendrite method for cluster analysis. Communications in Statistics-theory and Methods. 1974;3:1-27.
29. Chen J, Bittinger K, Charlson ES, Hoffmann C, Lewis J, Wu GD, et al. Associating microbiome composition with environmental covariates using generalized UniFrac distances. Bioinformatics. 2012;28:2106-13.
30. Segata N, Izard J, Waldron L, Gevers D, Miropolsky L, Garrett WS, et al. Metagenomic biomarker discovery and explanation. Genome Biol. 2011;12:R60.
31. Asnicar F, Weingart G, Tickle TL, Huttenhower C, Segata N. Compact graphical representation of phylogenetic data and metadata with GraPhlAn. PeerJ. 2015;3:e1029.
32. Sverrild A, Kiilerich P, Brejnrod A, Pedersen R, Porsbjerg C, Bergqvist A, et al. Eosinophilic airway inflammation in asthmatic patients is associated with an altered airway microbiome. J Allergy Clin Immunol. 2017;140:407-17.e11.
33. Son JH, Kim JH, Chang HS, Park JS, Park CS. Relationship of Microbial Profile With Airway Immune Response in Eosinophilic or Neutrophilic Inflammation of Asthmatics. Allergy Asthma Immunol Res. 2020;12:412-29.
34. Singh AK, Stock P, Akbari O. Role of PD-L1 and PD-L2 in allergic diseases and asthma. Allergy. 2011;66:155-62.
35. Zdrenghea MT, Johnston SL. Role of PD-L1/PD-1 in the immune response to respiratory viral infections. Microbes Infect. 2012;14:495-9.
36. Rutting S, Thamrin C, Cross TJ, King GG, Tonga KO. Fixed Airflow Obstruction in Asthma: A Problem of the Whole Lung Not of Just the Airways. Front Physiol. 2022;13:898208.
37. Lee HY, Kang JY, Yoon HK, Lee SY, Kwon SS, Kim YK, et al. Clinical characteristics of asthma combined with COPD feature. Yonsei Med J. 2014;55:980-6.
38. Sin BA, Akkoca O, Saryal S, Oner F, Misirligil Z. Differences between asthma and COPD in the elderly. J Investig Allergol Clin Immunol. 2006;16:44-50.
39. Olaguibel Rivera JM, Alvarez-Puebla MJ, Puy Uribe San Martín M, Tallens Armand ML. Duration of asthma and lung function in life-long nonsmoking adults. J Investig Allergol Clin Immunol. 2007;17:236-41.
40. Sousa AW, Barros Cabral AL, Arruda Martins M, Carvalho CRF. Risk factors for fixed airflow obstruction in children and adolescents with asthma: 4-Year follow-up. Pediatr Pulmonol. 2020;55:591-8.
41. Castillo JR, Peters SP, Busse WW. Asthma Exacerbations: Pathogenesis, Prevention, and Treatment. J Allergy Clin Immunol Pract. 2017;5:918-27.
42. McEvoy CT, Le Souef PN, Martinez FD. The Role of Lung Function in Determining Which Children Develop Asthma. J Allergy Clin Immunol Pract. 2023;11:677-83.
43. Abdo M, Pedersen F, Kirsten AM, Veith V, Biller H, Trinkmann F, et al. Longitudinal Impact of Sputum Inflammatory Phenotypes on Small Airway Dysfunction and Disease Outcomes in Asthma. J Allergy Clin Immunol Pract. 2022;10:1545-53.e2.

44. Hastie AT, Mauger DT, Denlinger LC, Coverstone A, Castro M, Erzurum S, et al. Mixed Sputum Granulocyte Longitudinal Impact on Lung Function in the Severe Asthma Research Program. Am J Respir Crit Care Med. 2021;203:882-92.
45. Hofstra JJ, Matamoros S, van de Pol MA, de Wever B, Tanck MW, Wendt-Knol H, et al. Changes in microbiota during experimental human Rhinovirus infection. BMC Infect Dis. 2015;15:336.
46. Singleton TE, Massari P, Wetzler LM. Neisserial porin-induced dendritic cell activation is MyD88 and TLR2 dependent. J Immunol. 2005;174:3545-50.
47. Jackson DJ, Gern JE. Rhinovirus Infections and Their Roles in Asthma: Etiology and Exacerbations. J Allergy Clin Immunol Pract. 2022;10:673-81.
48. Powell EA, Fontanella S, Boakes E, Belgrave D, Shaw AG, Cornwell E, et al. Temporal association of the development of oropharyngeal microbiota with early life wheeze in a population-based birth cohort. EBioMedicine. 2019;46:486-98.
49. Larsen JM, Steen-Jensen DB, Laursen JM, Søndergaard JN, Musavian HS, Butt TM, et al. Divergent pro-inflammatory profile of human dendritic cells in response to commensal and pathogenic bacteria associated with the airway microbiota. PLoS One. 2012;7:e31976.
50. Larsen JM, Musavian HS, Butt TM, Ingvorsen C, Thysen AH, Brix S. Chronic obstructive pulmonary disease and asthma-associated Proteobacteria, but not commensal Prevotella spp., promote Toll-like receptor 2-independent lung inflammation and pathology. Immunology. 2015;144:333-42.
51. Thorsen J, Rasmussen MA, Waage J, Mortensen M, Brejnrod A, Bønnelykke K, et al. Infant airway microbiota and topical immune perturbations in the origins of childhood asthma. Nat Commun. 2019;10:5001.
52. Lee SY, Mac Aogáin M, Fam KD, Chia KL, Binte Mohamed Ali NA, Yap MMC, et al. Airway microbiome composition correlates with lung function and arterial stiffness in an age-dependent manner. PLoS One. 2019;14:e0225636.
53. Chiu CY, Cheng ML, Chiang MH, Wang CJ, Tsai MH, Lin G. Integrated metabolic and microbial analysis reveals host-microbial interactions in IgE-mediated childhood asthma. Sci Rep. 2021;11:23407.
54. Beauruelle C, Guilloux CA, Lamoureux C, Héry-Arnaud G. The Human Microbiome, an Emerging Key-Player in the Sex Gap in Respiratory Diseases. Front Med (Lausanne). 2021;8:600879.
55. Mac Aogáin M, Ali NABM, Tsang A, Lee S, Fam KD, Yap M, et al. Age-associated change in respiratory microbiome architecture in healthy Singaporean subjects. Eur Respir J. 2019;54:PA2690.

Manuscript received January 17, 2023; accepted for publication May 24, 2023.

Myung Hyun Sohn

Department of Pediatrics
Severance Hospital
Institute of Allergy, Brain Korea 21 PLUS Project for Medical Science
Yonsei University
College of Medicine, Seoul, Korea
E-mail: mhsohn@yuhs.ac